© 2021. Published by The Company of Biologists Ltd | Journal of Experimental Biology (2021) 224, jeb239442. doi:10.1242/jeb.239442

RESEARCH ARTICLE

Tactile active sensing in an insect plant pollinator

Tanvi Deora*, Mahad A. Ahmed, Thomas L. Daniel and Bing W. Brunton

ABSTRACT

The interaction between insects and the flowers they pollinate has driven the evolutionary diversity of both insects and flowering plants, two groups with the most numerous species on Earth. Insects use vision and olfaction to localize host plants, but we know relatively little about how they find the tiny nectary opening in the flower, which can be well beyond their visual resolution. Especially when vision is limited, touch becomes crucial in successful insect–plant pollination interactions. Here, we studied the remarkable feeding behavior of crepuscular hawkmoths *Manduca sexta*, which use their long, actively controlled, proboscis to expertly explore flower-like surfaces. Using machine vision and 3D-printed artificial flower-like feeders, we revealed a novel behavior that shows moths actively probe surfaces, sweeping their proboscis from the feeder edge to its center repeatedly until they locate the nectary opening. Moreover, naive moths rapidly learn to exploit these flowers, and they adopt a tactile search strategy to more directly locate the nectary opening in as few as three to five consecutive visits. Our results highlight the proboscis as a unique active sensory structure and emphasize the central role of touch in nectar foraging insect–plant pollinator interactions.

KEY WORDS: Mechanosensory feedback, Tactile sensing, Proboscis, Hawkmoth, Learning

INTRODUCTION

Insect–plant pollination interactions have shaped the spectacular diversity of both plants and insects. The ability of insects to pollinate flowering plants has been one of the forces driving the rapid evolutionary diversification of angiosperms (Grimaldi, 1999; Crepet, 1996; Kay and Sargent, 2009). Further, flowering plants constitute the majority of human agricultural produce and although 60% of the agricultural crop volume is produced by plants that do not require animal pollination, 92 out of 108 commodity crops (85% of the world's leading crops) have increased fruit or seed set with animal pollination (Klein et al., 2007). More importantly, animal pollinated flowering plants constitute 87.5% of species-level diversity in flowering plants globally (Ollerton et al., 2011). Hence, pollination also serves a core ecological service, maintaining the functional integrity of these ecosystems and thus is crucial for sustainable agricultural production for human populations today. Over millions of years, the co-evolution of insects and flowering plants has produced a stunning variety of floral specializations. Flowers display species-specific olfactory and visual cues to attract both generalist and specialist insects; insects, in turn, use these cues to find and pollinate their host plants as has been shown in a series of key papers in the field (Raguso and Willis, 2005; Goyret et al., 2008a; Riffell et al., 2013, 2009; Kelber, 1997, 2002).

For successful feeding and pollination, insects need to not only identify and localize their host flower but also detect the tiny nectary opening on the floral surface. For insects like moths and butterflies, this task is particularly difficult, as they hover in front of the flower to access the nectary with their long, flexible, straw-like mouthpart known as the proboscis. Moreover, crepuscular hawkmoths like *Manduca sexta* are active in dim light conditions at dawn and dusk, when visual feedback is limited by long neural delays (Theobald et al., 2009; Stöckl et al., 2020, 2016; Sponberg et al., 2015). In addition, the visual resolution of moths at about a proboscis length away at dawn/dusk light levels is of the order of a few centimeters, whereas the nectary opening is no larger than a few millimeters (Stöckl et al., 2020; Theobald et al., 2009). Therefore, tactile feedback can be especially important for insects like moths and butterflies to successfully target the tiny flower nectary opening as they hover over the flowers. Few studies have focused on the role of rapid and precise mechanosensory feedback in this pollination interaction.

Several papers have demonstrated that the shape and texture of floral surfaces provide both visual and mechanosensory cues in pollination interactions (Goyret and Raguso, 2006; Goyret, 2010; Goyret et al., 2008b; Goyret and Kelber, 2011, 2012; Campos et al., 2015; Peng et al., 2019). These studies used artificial flower-like feeders of varying sizes and shapes to show that the success of hawkmoths in emptying the flower largely depends on the surface area of the feeder and whether tactile features such as grooves were present (Goyret and Raguso, 2006). This observation was true not only for physical grooves but also for visually contrasting stripes on the feeder surfaces (Goyret, 2010). Moreover, these tactile and visual floral features helped moths improve their performance over repeated visits, enabling them to learn to get to the nectary faster. The series of contributions in which Goyret and colleagues (Goyret, 2010; Goyret and Kelber, 2012) reported observations about a range of proboscis movements during pollination raised the important possibility that such movements could represent an active and systematic exploration of the floral surface, thus motivating our detailed machine vision-based quantitative analysis of proboscis movements.

The moth proboscis is a modified mouthpart that evolved from the two maxilla. When the moth first emerges from the pupal case, it unites the two galeae of the maxilla, and zips them together to form a central tube called the food canal, which serves as a drinking straw (Zhang et al., 2018). Both galeae are heavily muscularized and hydraulically controlled such that the proboscis is both flexible and actively actuated by muscles at its base and along its length (Wannenmacher and Wasserthal, 2003). The galeae of the proboscis are lined with muscles and also carry the trachea and the nerve cord. During flight, the proboscis is usually held curled up under the head. However, as a moth approaches a flower, it unfurls its proboscis by pumping body fluid into the galeae. In addition to active control by muscles and hydraulic extension, the proboscis is covered by a vast

Department of Biology, University of Washington, Seattle, WA 98195, USA.

*Author for correspondence (tanvid2@uw.edu)

T.D., 0000-0002-4019-2882

Received 15 October 2020; Accepted 3 January 2021

Journal of Experimental Biology (2021) 224, jeb239442. doi:10.1242/jeb.239442

array of mechanosensory sensillae all along its length and at its base (Krenn, 1990, 2010). Thus, the proboscis is both a feeding structure and an actively actuated sensory organ whose mechanical properties can be tuned by muscle activation. Perhaps as a result in part to this complexity, direct quantification of proboscis movements has remained elusive. Previous work has identified a range of behaviors in which the animals explore different floral features and points to a strong role of active sensory exploration. In this paper, we combined these behaviors with machine vision, enabling a quantitative approach to understanding tactile strategies of floral exploration.

In particular, we studied how moths use their proboscis to probe floral-like surfaces when presented with different tactile cues. We asked whether moths passively move their proboscis along tactile gradients or actively deploy their sensory proboscis to acquire tactile cues that might lead to the nectary. In addition, we also explored the role of learning and quantified how the strategy used by moths to extract tactile features changes over repeated visits. We leveraged the natural feeding behavior of hawkmoths to develop a robust, automated behavioral paradigm where tactile cues on artificial feeders are determined by the curvature of their 3D-printed artificial corollas (henceforth referred to as artificial flower or feeder; Fig. 1A,B; see also Campos et al., 2015; Peng et al., 2019). We used computer vision to automate tracking of moths and proboscis tip movements as they visited and fed repeatedly from these artificial flowers in dim-light conditions, where the tiny opening of the nectary greatly exceeds their visual acuity (Fig. 1C). We found that moths use their proboscis to locate the nectary opening by systematically sweeping each flower from edge to center (Fig. 1D). Further, this active exploration improved rapidly, and moths learned a direct strategy to pinpoint the nectary opening after as few as

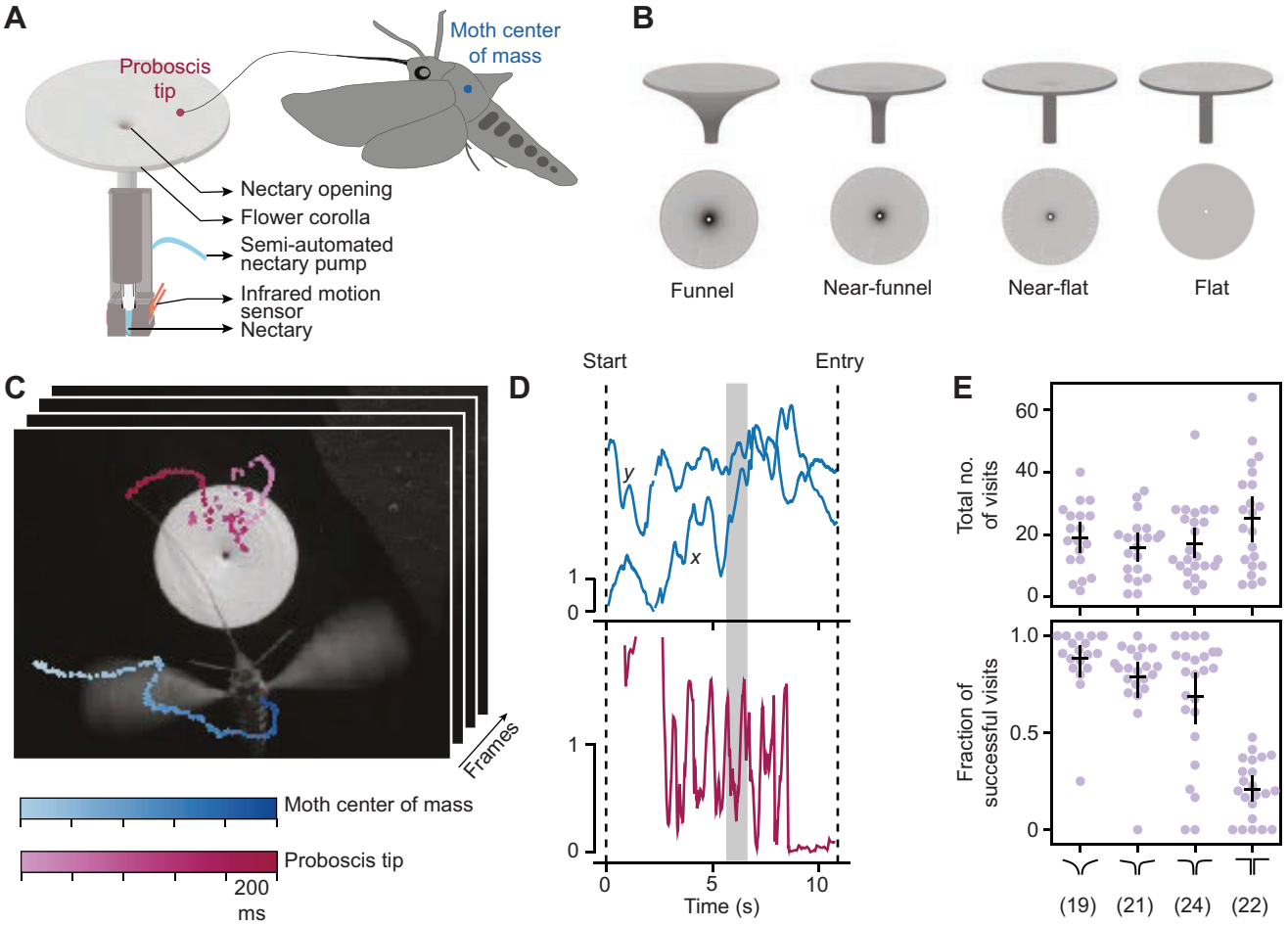

Fig. 1. Moths fed from an instrumented, 3D-printed artificial flower-like feeder as we tracked their body and proboscis tip positions over repeated visits. (A) Schematic diagram of a moth visiting an artificial flower. We tracked the proboscis tip and moth's body using a high-speed camera with infrared illumination at 100 frames s^{-1}. The artificial flower base was instrumented with an infrared motion sensor that was triggered when the proboscis reached the nectary. The nectary was also connected to a semi-automated pump that refilled it after each visit (Peng et al., 2019). (B) The four artificial flower shapes from the side (top) and from overhead (bottom). All nectary openings had the same diameter and height; artificial flowers differed only in the curvature of the their corolla. (C) One frame from a video overlaid with moth (blue) and proboscis tip (magenta) tracks on a near-flat flower. (D) Example of tracked trajectories for a single visit, showing the moth (blue) and proboscis tip (magenta) position. The moth position is shown in global coordinates relative to the camera view. The proboscis tip trajectory is shown as the radial distance relative to the center of the nectary opening on the artificial flower. The gray bar highlights the time window shown in C. The two dashed lines mark exploration time, defined as the start of a visit ('Start') and the time at which the proboscis entered the nectary opening ('Entry'). The scale bars represent one flower radius (25 mm). (E) The total number of visits (top) and the fraction of successful visits (bottom) across different floral shapes. The total number of visits was not different across the floral shapes (Kruskal–Wallis *H*-test P=0.24); however, the fraction of successful visits was dependent on floral shape (Kruskal–Wallis *H*-test P=4.21e−09, pairwise Tukey HSD P<0.05 for funnel/near-flat, funnel/flat, near-funnel/flat and near-flat/flat pairs). Each dot represents an individual moth; black lines represent the mean and s.d. The numbers in parentheses are the total number of moths that interacted at least once with each floral shape.

Journal of Experimental Biology

three to five consecutive visits of the same flower. These results demonstrate the role of active tactile exploration in flower feeding and pollination and a capacity in moths to both acquire relevant tactile information and modify tactile exploration strategy with learning. Touch is a fundamental sensory perception used by all animals to accomplish complex motor behaviors, and it serves a vital role in coordinating the seemingly effortless interactions between one's body and physical objects in the physical world (Saal and Bensmaia, 2014; Diamond and Arabzadeh, 2013). Understanding how touch shapes these interactions helps us understand a process of great ecological relevance and may also inspire novel haptic technologies.

MATERIALS AND METHODS

Moths

We used 2–5 days post-eclosion tobacco hawkmoth, *Manduca sexta* (Linnaeus 1763), from a colony maintained at the University of Washington. Moths were maintained on a 12 h:12 h light:dark cycle. Adults that showed an eagerness to feed, as assessed by the fact that they flew and hovered in front of a red LED headlamp with their proboscis extended, were selected for experiments. We used both male and female moths for our experiments (funnel-shaped feeder: 11 females and 8 males; near-funnel: 10 females, 10 males and 1 unknown; near-flat: 11 females, 12 males and 1 unknown; and flat: 11 females and 11 males). All moths were flower-naive and had never fed prior to experimentation. Moths were dark-adapted for at least 30 min before the experiment.

Behavioral setup

Experiments were conducted in an closed arena (~91×69×91 cm) with transparent acrylic walls covered by black cardboard. The entire arena was draped with a black cloth to ensure no external light entered the behavioral chamber. All experiments were performed during the active, night period of hawkmoths including dusk and dawn, at about 20–25°C. Three viewing windows were cut out of the cardboard to allow video recording and infrared illumination. A high-speed camera (Basler piA640-210gm GigE) was mounted on top of the behavioral chamber and was illuminated using three infrared LED panels. Infrared light is invisible to moths, and hence we used an additional white LED headlamp with a diffuser on one edge of the chamber to simulate dusk/dawn conditions of ~0.1–1 lx at the flower surface, measured using a light meter (Gossen Mavolux 5032C).

We mounted an artificial, 3D-printed feeder equipped with micro-sensors (see below) under the camera view. In addition, another funnel-shaped distractor feeder was placed in the same arena to distract the moths from the rewarded feeder between distinct visits. The distractor feeder had an empty nectary reserve and moths never received reward for visiting it.

Artificial flowers

Each moth was presented with one of four artificial flower shapes. The shape of the 3D-printed flower-like corolla was parameterized by the following equation, expressed in cylindrical coordinates (Campos et al., 2015):

$$z(r) = L\left(\frac{r - r_o}{R}\right)^{e^c}, \quad (1)$$

where $z(r)$ is the longitudinal axis of the flower, and r is the radial axis of the corolla from the central z-axis. Each corolla shape is then specified by 4 parameters: r_o=1 mm is the radius of the nectary opening, R=25 mm is the radius of the corolla, L=25 mm is the length of the flower, and c is a curvature parameter determining the lateral profile of the corolla.

We varied the exponent c to generate artificial flowers of different corolla curvature; the funnel, near-funnel, near-flat and flat flower had c=−1, −2, −3 and ∞, respectively. Feeder corollas were 3D printed using white PLA on a UPrint printer. Despite high printer resolution, the flower surface had regular concentric grooves from printing layers. We sanded and polished the surface using a rotary tool (Dremel 300 series) to provide a smooth surface. The base of the 45 mm long stalk housed a 200 µl PCR tube that served as the nectary reserve (henceforth referred to as the nectary; design files can be found at https://github.com/TanviDeora/FlowerDesigns). We filled the nectary with 25 µl of 20% sucrose using a semi-automated, custom-built nectary pump at the start of the experiment and also between moth visits (Peng et al., 2019; design files can be found at https://github.com/jgsuw/microinjector). Two thin copper wires along the length of the nectary tube detected the presence of nectar (sucrose solution). When the nectary was emptied, we prompted the pump to refill the nectary. Additionally, an infra-red transmitter and receiver pair were placed peripheral to the nectary to detect any motion inside the nectary itself. When the moth inserted its proboscis inside the nectary, the light beam became interrupted and the motion was then recorded by a custom-written MATLAB script (Arduino and MATLAB codes used can be found at https://github.com/TanviDeora/Arduino-control-codes-for-flight-rig and https://github.com/TanviDeora/MotionVideoCapture, respectively). After a successful feeding, if the moth reappeared at the artificial flower in less than 6 s, it was not considered as a new visit and the moth was not rewarded with nectar. Because our camera view was zoomed in to view the feeder surface, we empirically established this time interval to ensure that the moth had indeed finished the visit and did not reappear in the camera view, and we avoided refilling the nectary reserve while the moth proboscis was inside the feeder.

Video tracking

To maintain moths in a motivated state, we used a 7-component scent mixture that mimicked the scent of flowers pollinated by hawkmoths (Campos et al., 2015; the mixture of volatiles was 0.6% benzaldehyde, 17.6% benzyl alcohol, 1.8% linalool, 24% methyl salicylate, 3% nerol, 9% geraniol, 0.6% methyl benzoate in mineral oil). A few drops of this scent were placed on filter paper and positioned above the rewarded artificial flower on the ceiling of the chamber. We released the moth at one end of the chamber on a raised platform and allowed it to feed repeatedly for a maximum of 30 min. The camera captured video at 100 Hz, with 200 µs exposures, and was time synced with the infrared motion sensor and pump. If a moth failed to interact with the feeder within the first 10 min, the experiment was concluded and the moth was removed from further experiments and analysis. For all artificial flower shapes, we analyzed only those moths that interacted with the flower at least once.

Analysis of moth learning

We wrote custom Python scripts (https://github.com/TanviDeora/MothLearning) and used background subtraction to detect the center of mass (moth) and to extract all the instances when the moth appeared in our camera view. The moth and proboscis tip were also tracked by using a trained neural network (DeepLabCut; Mathis et al., 2018). In some cases, the moth would fly across the camera view without interacting with the flower, often with the proboscis coiled. To identify these false visits, we manually labeled a subset of the visits as true/false, and computed the visit duration for each

Journal of Experimental Biology (2021) 224, jeb239442. doi:10.1242/jeb.239442

category. We used these data to empirically set the threshold to 1.5 s in order to identify the true visits. This interval was also computed using a support vector machine-based supervised classification on the labeled visits mentioned above. Additionally, we computed the mean likelihood of tracking the proboscis tip in true visits for these labeled visits. Taken together, we classified each instance of moth appearance as a visit if the moth was in view for longer than 1.5 s and if the mean likelihood of tracking the proboscis tip was greater than 0.4 (based on DeepLabCut tracking). Finally, as mentioned earlier, all visits less than 6 s apart were merged to be counted as a single visit.

Using the time-synced motion sensor data from the nectary, we computed exploration time as the time difference between when the proboscis was detected to have entered the nectary and the start of the visit (Fig. 1). All successful visits were used for learning analyses. For each flower type, we fitted an exponential decay trend line of the form $y=a_0\exp(v/v_0)+y_0$ to explain how exploration time changed with visit number v for each flower shape. Because the exploration time data are noisy and this exponential decay trend line is sensitive to overfitting to outliers, we estimated y_0 (the asymptotic exploration time after learning) by averaging the last quarter of the data and used the average first-visit exploration time as a_0. The data shown in Fig. 2 were then used to fit v_0 by minimizing root mean square error (see also Fig. S1).

We used the exploration times of all moths from their early visits (visits 1–3) and later visits (visits 20–30) to estimate probability density functions (PDFs) using a Gaussian kernel density estimator in SciPy. Visits from all moths were pooled for this analysis, because there were too few visits from each moth (n=4 visits on average per moth per condition) to estimate PDFs or to model

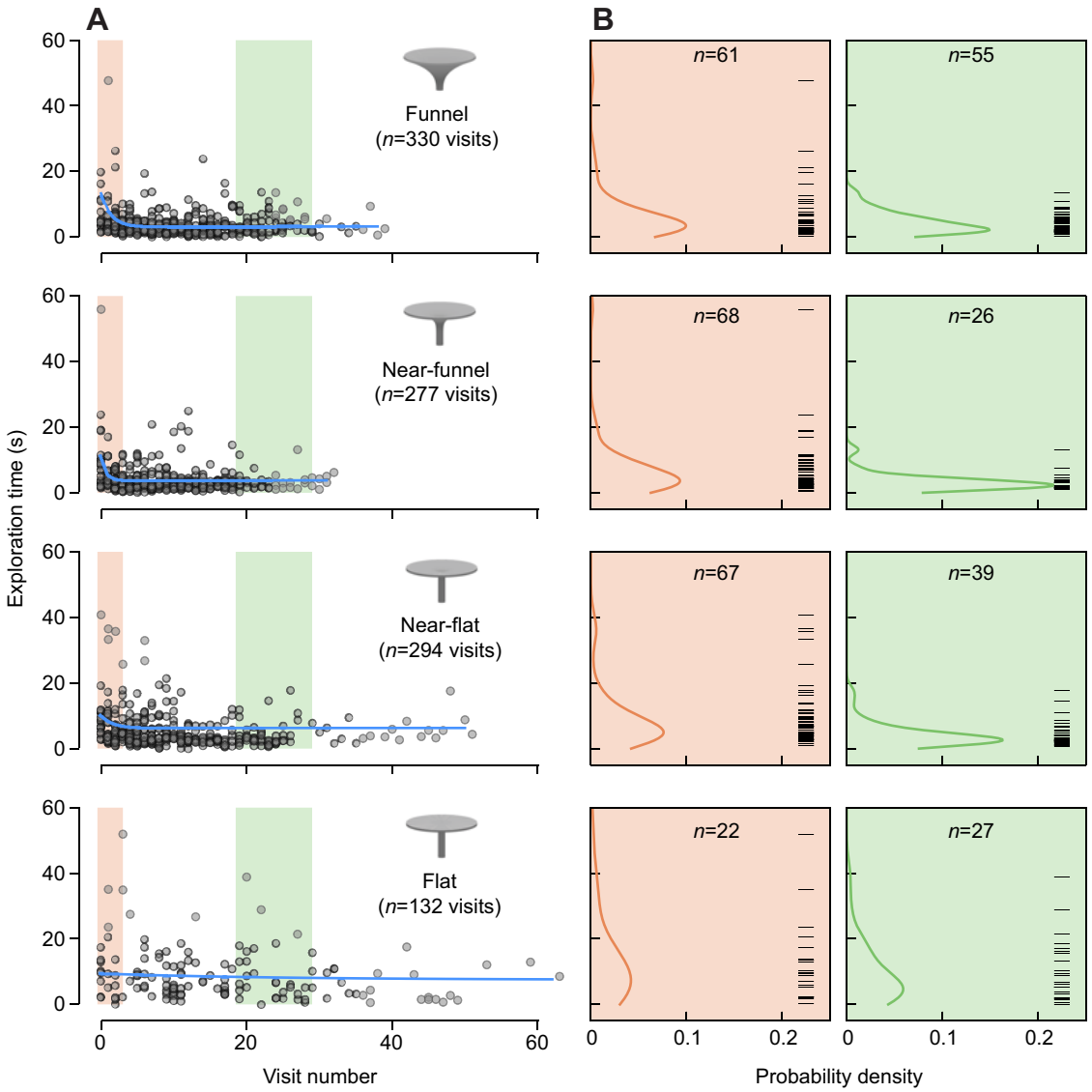

Fig. 2. Moths learn to handle artificial flowers in a shape-dependent manner. (A) Learning curves for the four different floral-like artificial flower shapes. Each gray dot is the exploration time for a single, successful visit. The blue solid curve shows the exponential fit to the data. *n* is the number of successful visits pooled across all moths for each flower shape. Visits were pooled across all moths that interacted with the flower even once (as shown in Fig. 1E); *N*=19, 21, 24 and 22 moths for funnel, near-funnel, near-flat and flat flowers, respectively. The exploration times for the early (visits 1–3, orange) and late (visits 20–30, green) visits were pooled and compared, as shown in B. (B) Probability density estimations of exploration time for early (orange) and late (green) visits. The black ticks on the right in each panel show a raster plot of the raw data used to fit the probability density curves. *n* represents the total number of visits, pooled across all moths that successfully visited the artificial flower.

individual effects explicitly. For visits 1–3 (orange), there were n=61 visits to funnel across 19 moths, 68 visits to near-funnel across 20 moths, 67 visits to near-flat across 21 moths, and 22 visits to flat across 14 moths. For visits 20–30 (green), there were n=55 visits to funnel across 9 moths, 26 visits to near-funnel across 5 moths, 39 visits to near-flat across 9 moths, and 27 visits to flat across 10 moths. We then used the Kolmogorov–Smirnov (KS) test to evaluate whether these PDFs were different from each other. In addition, we computed the Kullback–Leibler (KL) divergence (DKL) to quantify how the PDFs differ from the reference funnel-shaped PDF.

Proboscis kinematics

We tracked the tip of the unfurled proboscis, the base of the proboscis and the two antennae by training a neural network (DeepLabCut; Mathis et al., 2018). We used 825 manually annotated frames and trained for 1,030,000 iterations until convergence. To augment the training, a subset of the training data set included frames that were rotated to make the tracking performance rotation invariant.

We wrote custom Python scripts (https://github.com/TanviDeora/ProboscisTracking) to smooth the resultant tracking trajectories and to mitigate the impact of outliers on our analyses. We computed the distance between the proboscis tip in adjacent frames in manually annotated videos (videos for 6 visits across the 4 floral shapes). Based on this distribution of distances, we estimated the error cutoff to be 24 pixels and used this cutoff to filter DeepLabCut annotation, eliminating all jumps greater than this cutoff (Fig. S3). The resulting tracks were smoothed using a median filter (window size 11 time steps) and interpolated with a 3rd order polynomial. Some visits could not be tracked using DeepLabCut and were thus manually tracked.

Proboscis kinematics relative to the flower

We computed two kinematic variables from these tracked proboscis trajectories. First, the relative radial distance was computed as the distance of the proboscis tip from the center of the artificial flower normalized to the radius of the artificial flower. Second, the relative radial orientation (RRO) was computed as the angle between the proboscis tip trajectory and radial axis. The angle was wrapped to restrict the range to 0–90 deg. Although we quantified only the position of the proboscis tip, the moth used the entire length of the proboscis to touch the artificial flower. Hence, even when the tip was not in contact with the feeder surface, some part of the proboscis behind the tip often was in contact. Therefore, to quantify sweeping behavior, we also included data for locations that were >1 but <2 radial distances away from the center and calculated the number of peaks and frequency of sweeping for all proboscis tip trajectories. To compute the number of peaks, we used the Python SciPy function *find peaks* that uses the prominence (value=0.5) to find the local peaks from neighboring points. We computed frequency as the inverse of the time interval between successive peaks. All proboscis kinematic analysis was performed on visits 1, 7 and 20 for all moths across all flower shapes to compare exploration strategy across early visits and later visits (Fig. 2; for all shapes, the moths learned within 3–5 visits, visit 1 represents the first interaction, visit 7 is early learning, and visit 20 is later learning).

We also fitted Gaussian kernel estimations to estimate PDFs and used KL divergence to compare the distributions. To analyze relative radial orientation, we ignored parts of the trajectory very close to the center (r<0.06) because the RRO values close to the feeder center were ambiguous. We plotted tip trajectory distribution in 2D of relative radial distance and relative radial orientation as heat maps and hexbins. We also estimated the PDFs and contours by fitting 2D Gaussian kernels, using a kernel width that was 1.5 times the bandwidth estimated using Scott's rule.

Proboscis kinematics relative to the moth head

Moths keep their antennae stable at a constant angle during flight (Sane et al., 2007). Hence, to compute the head direction vector, we used the base of the proboscis (also the tip of the head) and the point perpendicular to the line joining the left and right antennae tip (Fig. S2). We computed the proboscis vector as the line joining the base and tip of the proboscis. The angle between the head direction vector and the proboscis vector was computed as the head–proboscis angle. The length of the proboscis vector represented the proboscis tip position relative to the head. The polar plots of the head–proboscis motion plots the head–proboscis angle along the theta axis and the proboscis tip position along the radial axis.

RESULTS

We studied the behavior of moths as they explored and learned to feed from artificial feeders of different flower-like shapes. In our behavioral paradigm, moths were allowed to feed from 3D-printed artificial flower-like feeders in a light-controlled chamber while we tracked their center of mass and the tip of their proboscis using a high-speed camera under infrared illumination (Fig. 1A,C). All moths were naive to the behavioral paradigm and had never fed from any flower (artificial or otherwise) before. Each artificial flower was equipped with a nectary reserve at its base, and this nectary reserve re-filled automatically following successful feeding, so that a single moth could visit the same feeder repeatedly. We presented each moth with one of four artificial flower shapes, which differed in the curvature of their corollas (Fig. 1B). Each naive moth was tested in a single 30 min session and with one feeder shape; the total number of visits across all feeder shapes was similar [Fig. 1E; Kruskal–Wallis (KW) H-test P=0.24; see Campos et al., 2015]. Consistent with previous findings (Campos et al., 2015), we found that the funnel-shaped feeder was the easiest to exploit and the flat feeder was the most difficult, as measured by the fraction of visits where the moth accomplished successful feeding over 30 min (Fig. 1E; KW H-test P=4.21e−09, pairwise Tukey HSD P<0.05 for funnel/near-flat, funnel/flat, near-funnel/flat and near-flat/flat pairs).

Moths learn to feed from different artificial flower shapes over repeated visits

We found that moths quickly learned over repeated visits to the same artificial flower to exploit the curvature of the feeder corolla, even when it was very slight, to locate the nectary (Fig. 2). We measured how long each moth spent exploring the artificial flower at each visit, defined as the time elapsed between when the moth first came into the camera view near the artificial flower and when its proboscis reached the base of the nectary reserve (Fig. 1C,D). In artificial flower shapes with slight curvature, we found that this exploration time decreased with repeated visits (Fig. 2; Table S1a; KS test P=1.05e−2 and P=2.41e–04 for near-funnel and near-flat, respectively, comparing early and late visits). For funnel-shaped artificial flowers, the exploration time did not decrease over time (KS test, P=0.546), consistent with our observation that funnel-shaped artificial flowers are easiest to exploit; moths found the nectary reserve on their first visit and repeated visits did not improve their efficiency. In contrast, for flat artificial flowers, the exploration time did not decrease over repeated visits, suggesting moths did not learn to handle artificial flowers that do not provide surface shape cues to the nectary opening's location (KS test P=0.463).

Although moths learned after 3–5 visits to handle all three curved artificial flowers, their early exploration times still depended on flower shape. As shown in Fig. 2, the aggregated probability densities of all early visits (1–3) varied in a flower shape-dependent manner: values for dissimilarly shaped artificial flowers were more different than those for similarly shaped artificial flowers (Table S1b: KS test P=0.992 for funnel/near-funnel, P=0.026 for funnel/near-flat, P=0.003 for funnel/flat; and P=0.069 for near-funnel/near-flat, P=0.01 for near-funnel/flat and P=0.128 for near-flat/flat). This flower shape-dependent pattern was also evident when we computed how much the distributions diverged from each other using KL divergence (KL divergence, D_{KL}, increases as the floral shape diverges: D_{KL}=0.053 funnel/near-funnel, D_{KL}=0.109 funnel/near-flat, D_{KL}=0.228 funnel/flat artificial flowers). After learning, however, the exploration times did not differ among all shapes except the flat artificial flower (Table S1c; KS test P=0.063 for funnel/near-funnel, P=0.39 for funnel/near-flat, P=0.14 for near-funnel/near-flat, P=0.014 for flat/funnel, P=2.266e−4 for flat/near-funnel and P=2.93e–3 for flat/near-flat). Taken together, our data show that moths learn to handle novel artificial flowers that have even slight curvatures within as few as 3–5 visits. This is consistent with previous literature reporting learning in hawkmoths on artificial flowers of different size and texture (Goyret and Raguso, 2006; Goyret, 2010; Goyret and Kelber, 2011).

Moths actively sweep their proboscis to probe artificial flower surfaces

Tracking the tip of the moth proboscis revealed how these mouthparts were used to explore the floral-like surfaces of artificial feeders, by tapping and sweeping, as well as bending the proboscis against the surface (Movie 1). To understand the role of the proboscis in flower surface exploration, we trained a neural network to track the proboscis tip in high-speed videos (Mathis et al., 2018). We found that moths explored the feeder surface more extensively when attempting to feed from artificial flowers that were more difficult to exploit (Fig. 3A). These behaviors suggest that moths extract mechanical cues during interactions with the artificial flowers.

We next asked whether the moth moved its proboscis tip randomly over the surface, passively pushing it along mechanical gradients like the flower curvature until it found the nectary opening, or whether the moth actively actuated the tip to extract mechanical cues about the flower surface. To disambiguate these possibilities, we examined a few kinematic parameters computed from the proboscis tip tracking. First, we computed the position of the proboscis tip relative to the center of the artificial flower (Fig. 3C). We found that moths systematically and repeatedly swept their proboscis between the artificial flower edge and the center as they explored the surface (Fig. 3B). Moths moved their proboscis in radial sweeping motions, not just along the passive mechanical gradient from edge to center but also against the gradient from center to edge. The frequency of sweeps was 1.76 Hz (median, 25th and 75th interquartile range, IQR, of 1.12–2.86 Hz) for all moths and all floral shapes, during earlier and later visits (Fig. 3E). Moths found the nectary opening in fewer sweeps for artificial flowers with even slight curvature as compared with the flat flower (Fig. 3D; KW H-test P=8.65e−06). However, the number of sweeps did not show systematic and interpretable changes over repeated visits. For most shapes, as moths learned to handle these artificial flowers, they found the nectary opening within just a few sweeps. Interestingly, for the most challenging flat flower, moths continued to sweep multiple times for the later visits. These observations are consistent with the results above (Fig. 2) that moths did not learn to feed efficiently from completely flat flowers, despite repeated visits.

Moths could move their proboscis on the feeder surface by two physical mechanisms. First, they can move their entire body and drag the proboscis as it hovers over the artificial flower (Movie 1). Second, they can actuate the proboscis muscles that allow movement of the proboscis independent from that of the head and body of the moth. Although it is clear from direct observations and videos that moths do the former (Goyret, 2010; Goyret and Kelber, 2012), the latter movements are smaller and harder to observe. To explore whether moths move their proboscis independently of their body, we computed the relative motion of the proboscis tip with respect to the head (Fig. S2). We found that moths can indeed change both the relative position and the relative angle of the proboscis tip with respect to the head during flower exploration. This suggests they use both whole-body movements and independent proboscis movements to enable active sweeping motion on the floral surface.

Then, we examined the RRO of the proboscis tip with respect to the circular corolla of the artificial flower. RRO was defined as the angle between the proboscis tip trajectory and the flower's radial axis (Fig. 4A). In other words, if the proboscis is sweeping along the flower's radial axis, the RRO would be 0 deg, whereas sweeping perpendicular to the flower's radial axis would give RRO=90 deg. Exploring along the radial axis would inform moths about the feeder's curvature, leading toward the nectary opening at the center. Exploring perpendicular to the radial axis would not be informative about the artificial flower's surface, except at the edges, where it would inform the moth about the flower's outer shape.

Moths preferentially learn to acquire tactile features

As moths learned to exploit difficult artificial flowers, their exploration strategy shifted. This shift in strategy is best represented as shifts in probability density of the proboscis tip trajectories in two dimensions, RRO and relative radial position (Fig. 4). During the first visit, moths spent time exploring along the edge of the feeder in all flower shapes, as seen by the high probability density around one flower radius and with RRO=90 deg. For the easiest flower shape, across all visits, moths learned to directly find the nectary with only cursory exploration of the surface. This is evident by the high-density regions at a radial position of 0 and along all RRO in funnel and near-funnel flowers. For more difficult flower shapes of near-flat and flat flowers, on their first visit, moths explored the interior surface more extensively, at all radial orientations. However, with repeated visits, moths preferentially learned to explore along the radial axis. This radial mode of exploration is evident as the higher density shifts along RRO=0 deg for the later visits (visits 7 and 20) for both the near-funnel and near-flat flower. This shift is absent in both the easiest funnel shaped flower and also for the most difficult, flat flower, consistent with the fact that the flat flower has no information about the nectary opening location along the radial axis.

DISCUSSION

In summary, our results show that moths use their actively controlled and highly sensed proboscis to explore the 3D surface of artificial flowers as they locate the nectary opening. By high-speed video tracking of proboscis tip trajectories, we characterized how moths systematically swept their proboscis on artificial flowers, from edge to center and center to edge, as they explored novel floral shapes. Interestingly, as moths learned to exploit the corolla-like feeder curvature over repeated visits, they are able to find the nectary

Journal of Experimental Biology (2021) 224, jeb239442. doi:10.1242/jeb.239442

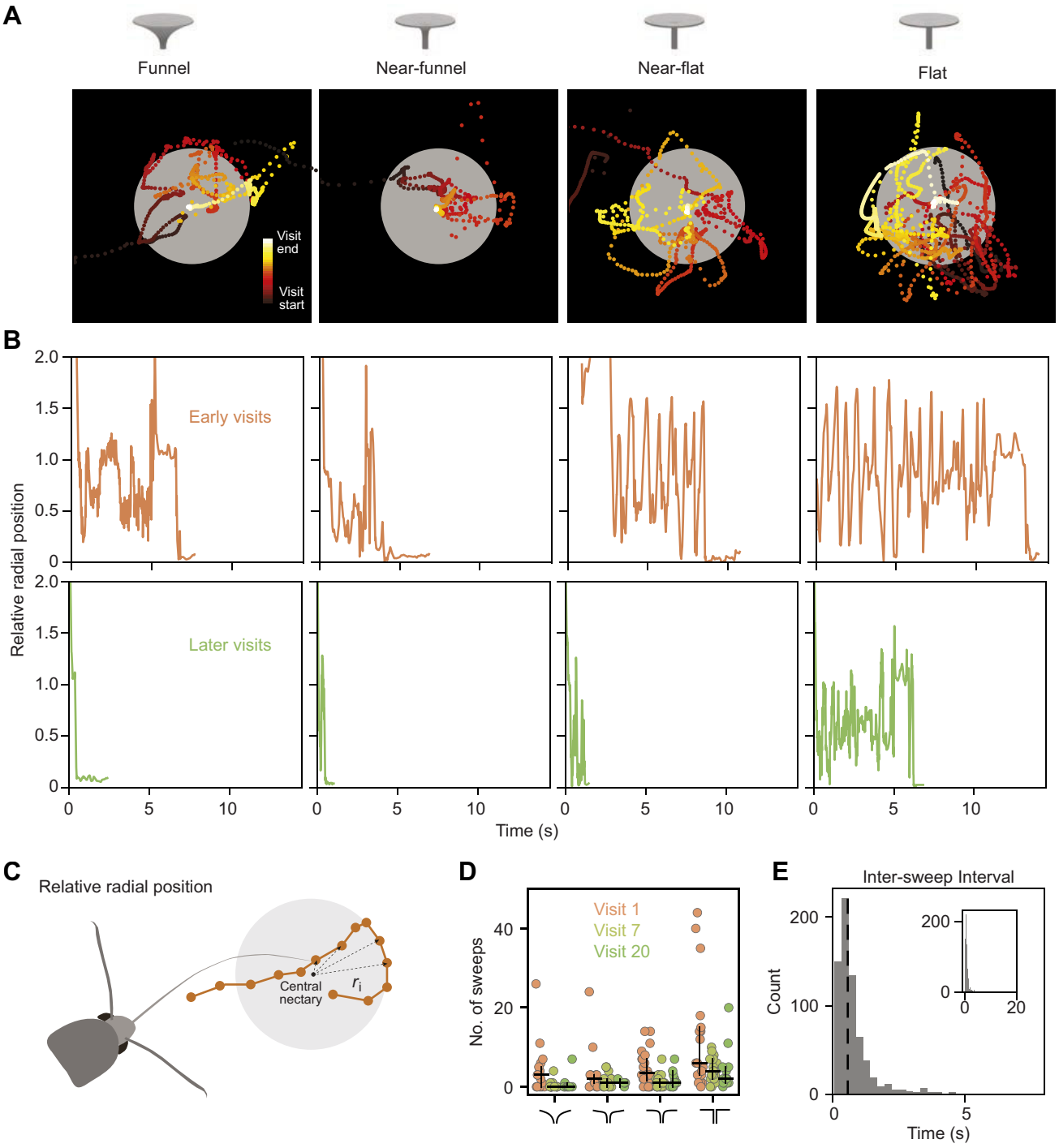

Fig. 3. Moths actively explore the feeder surface by sweeping their proboscis along the artificial flower. (A) The proboscis tip trajectory for a representative visit for each floral shape, color coded by time. (B) The relative radial position of the proboscis tip over time, showing that for all floral shapes, the moths swept from edge to center and center to edge repeatedly until they found the nectary for early and later visits. (C) Illustration of a proboscis trajectory (brown) and the corresponding position relative to the artificial flower radius (relative radial position, r_i) at certain locations on the trajectory. (D) The number of sweeps for all moths across the different floral shapes for the early visit (visit 1) and later visits (visit 7 and visit 20). Each dot represents a single visit for an individual moth; black lines represent the median and 95% CI. Visit 1: funnel N=16, near-funnel N=17, near-flat N=22, flat N=20; visit 7: funnel N=13, near-funnel N=16, near-flat N=20, flat N=17; visit 20: funnel N=8, near-funnel N=5, near-flat N=9, flat N=13 moths. The following outliers were not shown to ensure clarity: visit 1: near-funnel flower N=55 and flat flower N=83 moths. (E) A histogram showing the time interval between successive sweeps. The dashed line marks the median time interval of 0.56 s, which corresponds to a frequency of 1.76 Hz (25th and 75th interquartile range, IQR: 1.12–2.86 Hz). The inset shows the zoomed out plot.

opening within a few sweeps. Our results suggest that moths use active tactile sensing and learn an efficient strategy over visits to preferentially extract salient mechanical features of the floral edge and curvature.

Active tactile sensing

A variety of other insects are also known to use tactile feedback to interact with objects in the physical world (Erber et al., 1998; Schütz and Dürr, 2011; Comer et al., 2003; Camhi and Johnson, 1999). For

Journal of Experimental Biology (2021) 224, jeb239442. doi:10.1242/jeb.239442

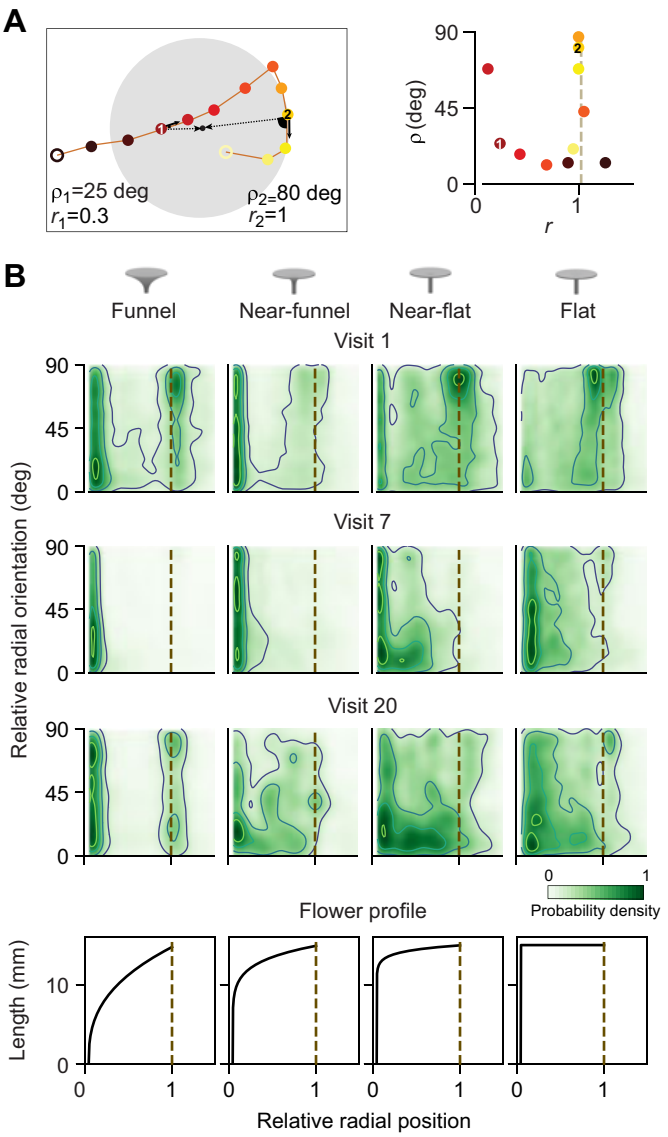

Fig. 4. Moths preferentially extract tactile features as they learn to feed from the novel artificial flower. (A) Left: an illustration of a proboscis trajectory (in orange) with discrete proboscis tip positions denoted by colored circles (color coded in time as in Fig. 3A) on an artificial flower surface with a central nectary opening (small black dot). The relative radial orientation (ρ) and relative radial position (*r*) are shown for two positions (1 and 2, as indicated) along the cartoon proboscis trajectory. The dotted line represents the radial axis and the black arrows represent the tangent along the proboscis trajectory at two representative positions. Right: location of the proboscis tip positions on heat map plots, like those shown in B. (B) Heat map of the proboscis tip as a function of relative radial orientation, and relative radial position for the four floral shapes (indicated above the panels) and over repeated visits (visits 1, 7 and 20), pooled across all moths. Peaks in probability density (see green scale) indicate moths preferentially explored the edges of the artificial flower (around radial position=1 and RRO=90 deg). In the interior of the artificial flower, the moths explored at all angles for the first visit. However, over repeated visits, the higher probability density shifted (green) along the radial axis (RRO=0 deg) for near-funnel and near-flat flowers. Visit 1: funnel *n*=6796 frames, *N*=16 moths; near-funnel *n*=10,086 frames, *N*=17 moths; near-flat *n*=10,214 frames, *N*=22 moths; flat *n*=25,729 frames, *N*=20 moths. Visit 7: funnel *n*=2278 frames, *N*=13 moths; near-funnel *n*=2979 frames, *N*=16 moths; near-flat *n*=2535 frames, *N*=20 moths; flat *n*=6729 frames, *N*=17 moths. Visit 20: funnel *n*=1727 frames, *N*=8 moths; near-funnel *n*=535 frames, *N*=5 moths; near-flat *n*=1429 frames, *N*=9 moths; flat *n*=5526 frames, *N*=13 moths.

instance, bees use their antennae and legs to detect the texture of floral surfaces (Kevan and Lane, 1985; Solvi et al., 2020). Unlike the smooth lower petal surfaces, the upper (adaxial) petal surfaces are covered in conical epidermal cells (Whitney et al., 2011). These conical cells influence petal color and reflectance, scent release and petal wettability, in addition to providing a rough, frictional texture surface for use during landing. Moreover, these conical epidermal cells are often arranged in a characteristic spatial pattern that may serve as nectar guides (Kevan and Lane, 1985). Indeed, bees can be trained to identify specific textures (Whitney et al., 2009). Unlike bees, which land on flowers, hawkmoths like *M. sexta* hover as they feed, and thus far floral surface microstructures have not been considered useful for pollination by hovering insects (Kraaij and Kooi, 2019). Interestingly, our results show that moths can learn to preferentially extract salient mechanical features on the floral-like feeder surface. Taken with prior literature, we suggest that in addition the overall floral curvatures and macro-textures such as the grooves on the petals (Goyret, 2010), moths, like bees, might be able to interact with and may leverage micro-textures on the floral surface. The role of micro-textures as mechanosensory cues in guiding hovering insect feeding remains relatively less explored (Policha et al., 2016).

Touch is a ubiquitous sensory modality across the animal kingdom, and a key feature of tactile sensing is active, and often rhythmic, movement of the sensor to probe and manipulate objects. For example, humans move our fingers to assess the texture of surfaces, and active finger movements lead to improved spatial resolution in touch (Skedung et al., 2013). The use of touch to assess objects and navigate one's environment has been well studied in diverse organisms, including insects, fish and rodents (Diamond et al., 2008; Erber et al., 1993; Camhi and Johnson, 1999; Mongeau et al., 2013). In fact, the rat whisker system is among the most well-studied examples of active tactile sensing (Diamond et al., 2008; Bush et al., 2016). Rats move their whisker bundle rhythmically to feel objects around them, helping them determine the shape and texture of objects and height of obstacles, to interact with other con-specifics and to navigate through their environment (Kleinfeld et al., 2006). Behaviorally, the moth's proboscis sweeping movements we observed are highly reminiscent of rat whisking.

Proboscis sensing and mechanics

Although the sweeping motion of the hawkmoth proboscis is very similar to the whisking motions of rat whiskers, the sensing and mechanics of the proboscis are entirely different. Rat whiskers are hair shafts of fixed mechanical stiffness, sensed at the base by a single sensory neuron and actuated by muscles at the base (Berg and Kleinfeld, 2003). Deflections of the whisker shaft can be uniquely mapped to mechanical forces and torques induced at the base of the whisker (Bush et al., 2016; Huet et al., 2015). The sensory neuron at the base can thus faithfully represent contact at the tip by responding to the forces and torques produced at the base. In contrast, the proboscis is hydraulically filled and has muscles not just at its base but along its entire length that actively control its motion, shape and structural mechanics (Krenn, 2010). Further, the proboscis has potential mechanosensors at its base and along its entire length. In its sensing and mechanics, the moth proboscis is closer to a muscular hydrostat, such as an elephant trunk or an octopus tentacle, except that the proboscis has a stiff cuticular exterior (Kier and Smith, 1985). How proboscis mechanics are controlled and how these deformations are sensed are fascinating open questions.

Although in our study we tracked only the proboscis tip, information about the surface would be encoded by potential

sensors at the proboscis base and also all along its length (Krenn, 1990, 2010). In addition to sweeping the proboscis tip along the surface, moths use other modes of sensing, such as bending the proboscis against the flower surface. Tracking the proboscis tip allowed us to quantify strategies of exploration with respect to the artificial flower shape (Figs 3 and 4). We also demonstrated how moths use both whole-body motions and independent actuation of the proboscis to expertly explore artificial flower surfaces (Fig. S2). However, the proboscis is very flexible, it is actuated at the base, and along its entire length. Specifically, the distal proboscis tip is extremely mobile and can be actuated at speeds much higher than the sweep frequencies that we report here. Moreover, it is interesting to note also that although the proboscis is not jointed, it has one relatively fixed point of flexion along its length (Movie 1). Further understanding of proboscis actuation would require expert tracking of the entire length of the proboscis in 3 dimensions.

Multisensory cues in flower exploration

In addition to tactile cues, moths may use feedback from various other sensory modalities to exploit real flowers and find the nectary. The visually contrasting grooves on flower surface provide cues that lead to the nectary, and moths have been shown to align their body along the nectar guides (Goyret, 2010; Goyret and Raguso, 2006). Even so, the visual resolution of moths is not sufficient to resolve the nectary opening or provide accurate feedback about proboscis motion. Vision can, however, enable detection of the outer flower contour (Roth et al., 2016; Stöckl et al., 2017). Thus, in addition to touch, the active movements of the proboscis might be also guided by vision, although with limited resolution (Stöckl et al., 2020; Goyret and Kelber, 2012). Indeed, moths handling flat artificial flowers continued to sweep from edge to center despite the lack of curvature cues (Fig. 3), even when very few visits were successful (Fig. 1).

Manduca sexta are crepuscular moths that are active during low-light conditions of dusk and dawn, so all of our experiments were conducted at low-light luminance. It is possible that light levels affect the visual control of proboscis motion. Indeed previous work suggests that the interaction of vision and touch may be even more crucial for diurnal moths (Goyret and Kelber, 2011) and butterflies in guiding precise proboscis motions. In addition to touch and vision, other sensory cues like humidity and CO_2 gradient over the corolla, as well as olfactory cues on the flower surface and nectary might also inform the active movements of the proboscis on natural flowers (Von Arx et al., 2012; Haverkamp et al., 2016; Goyret et al., 2008a; Kessler et al., 2015; Zhou et al., 2017). Moreover, other tactile features of natural flowers like the petal edges, texture on petals and even the orientation of the flower itself will likely influence the exploration strategy as well as learning capabilities (Haverkamp et al., 2019; Goyret, 2010; Goyret et al., 2008a).

Implications of learning and active sensing for pollination and diversity of flowering plants

The mechanistic processes underlying insect–plant pollination are shaped in large part by the insects' sensory systems and capacity for learning. For instance, bees can identify host plants and learn to associate color or odor with a reward, which influences how they exploit new nectar resources (Chittka and Raine, 2006). On an evolutionary time scale, these behavioral capabilities may also drive pollination syndromes (Johnson, 2012; Fenster et al., 2004). In other words, insect behavior may drive the evolution of certain floral traits, allowing specific insect species to specialize and exclusively pollinate specific plant species, and hence drive the evolution of new species. Our results show that the hawkmoth, an opportunistic insect that visits various different kinds of flowering plants, is also an exceptional learner and can learn to handle novel flowers within a few visits (Fig. 2; see also Goyret and Kelber, 2012). Experiments in the lab with artificial flowers reveal that the success of hawkmoths might not necessarily align with the best interests of the plant (Peng et al., 2019). Artificial flowers that are harder to exploit and more difficult for the insect pollinator to feed from may have greater success in transferring pollen (Peng et al., 2019), possibly as a consequence of increased handling time. Consistent with this literature, our results show that flat flowers have a lower success rate but moths spend more time exploring them, even with repeated visits (Figs 1 and 2). This mismatched interest, coupled with the hawkmoth's ability to learn and exploit relevant tactile cues in novel flowers, might have a profound impact on how they interact with flowers in the wild (Walton et al., 2020). That said, several other factors such as the time of day and orientation of the flower influence pollen transfer (Haverkamp et al., 2019; Fenske et al., 2018). Moreover, field studies reveal that the majority of the pollen load in hawkmoths is from flowers that are efficiently exploited by them (Alarcón et al., 2008). Future work using artificial flowers capturing additional floral features, as well as natural flowers, in addition to quantification of pollen transfer will help us understand the role of insect sensing and learning in shaping pollination interactions and, hence, floral diversity and insect forms over evolutionary time scales.

Acknowledgements

We would like to thank Joseph Sullivan for help with building the micro-sensor flower and nectary pump; John So for annotating videos; and Satpreet Singh and Pierre Karashchuk for help with video tracking. We especially thank Prof. Joaquin Goyret for both critical feedback and inspiration. We thank Ali Weber and Ajinkya Dahake for critical feedback on earlier versions of the manuscript.

Competing interests

The authors declare no competing or financial interests.

Author contributions

Conceptualization: T.D., T.L.D., B.W.B.; Methodology: T.D., T.L.D., B.W.B.; Formal analysis: T.D.; Investigation: T.D., M.A.A.; Data curation: T.D., M.A.A.; Writing - original draft: T.D.; Writing - review & editing: T.D., M.A.A., T.L.D., B.W.B.; Visualization: T.D., T.L.D., B.W.B.; Supervision: T.L.D., B.W.B.; Project administration: T.L.D.; Funding acquisition: T.D., T.L.D.

Funding

This work was funded by a Human Frontier Science Program Long-Term Fellowship to T.D., Washington Research Foundation Innovation Undergraduate Fellowship in Neuroengineering to M.A.A., the Komen Endowed Chair to T.L.D. and grants FA9550-14-1-0398 to T.L.D. and FA9550-19-1-0386 to B.W.B. from the Air Force Office of Scientific Research.

Data availability

Data are available from the Dyrad digital repository (Deora et al., 2021): dryad.sxksn030t. Design files (https://github.com/TanviDeora/FlowerDesigns; https://github.com/jgsuw/microinjector), Arduino and MATLAB codes (https://github.com/TanviDeora/Arduino-control-codes-for-flight-rig; https://github.com/TanviDeora/MotionVideoCapture), and custom-written Python scripts (https://github.com/TanviDeora/MothLearning and https://github.com/TanviDeora/ProboscisTracking) are available from GitHub.

Supplementary information

Supplementary information available online at https://jeb.biologists.org/lookup/doi/10.1242/jeb.239442.supplemental

References

Alarcón, R., Davidowitz, G. and Bronstein, J. L. (2008). Nectar usage in a southern Arizona hawkmoth community. *Ecol. Entomol.* **33**, 503-509. doi:10.1111/j.1365-2311.2008.00996.x

Berg, R. W. and Kleinfeld, D. (2003). Rhythmic whisking by rat: retraction as well as protraction of the vibrissae is under active muscular control. *J. Neurophysiol.* **89**, 104-117. doi:10.1152/jn.00600.2002
Bush, N. E., Schroeder, C. L., Hobbs, J. A., Yang, A. E. T., Huet, L. A., Solla, S. A. and Hartmann, M. J. Z. (2016). Decoupling kinematics and mechanics reveals coding properties of trigeminal ganglion neurons in the rat vibrissal system. *eLIFE* **5**, e13969. doi:10.7554/eLife.13969
Camhi, J. M. and Johnson, E. N. (1999). High-frequency steering maneuvers mediated by tactile cues: Antennal wall-following in the cockroach. *J. Exp. Biol.* **202**, 631-643.
Campos, E. O., Bradshaw, H. D. and Daniel, T. L. (2015). Shape matters: corolla curvature improves nectar discovery in the hawkmoth Manduca sexta. *Funct. Ecol.* **29**, 462-468. doi:10.1111/1365-2435.12378
Chittka, L. and Raine, N. E. (2006). Recognition of flowers by pollinators. *Curr. Opin. Plant Biol.* **9**, 428-435. doi:10.1016/j.pbi.2006.05.002
Comer, C. M., Parks, L., Halvorsen, M. B. and Breese-Terteling, A. (2003). The antennal system and cockroach evasive behavior. II. Stimulus identification and localization are separable antennal functions. *J. Comp. Physiol. A Neuroethol. Sens. Neural Behav. Physiol.* **189**, 97-103. doi:10.1007/s00359-002-0384-9
Crepet, W. L. (1996). Timing in the evolution of derived floral characters: Upper Cretaceous (Turonian) taxa with tricolpate and tricolpate-derived pollen. *Rev. Palaeobot. Palynol.* **90**, 339-359. doi:10.1016/0034-6667(95)00091-7
Deora, T., Ahmed, M., Daniel, T. and Brunton, B. (2021). Tactile active sensing in an insect plant pollinator. *Dryad Dataset.* doi:10.5061/dryad.sxksn030t
Diamond, M. E. and Arabzadeh, E. (2013). Whisker sensory system - From receptor to decision. *Prog. Neurobiol.* **103**, 28-40. doi:10.1016/j.pneurobio.2012.05.013
Diamond, M. E., Heimendahl, M. V. and Knutsen, P. M. (2008). ' Where' and 'what' in the whisker sensorimotor system. *Nat. Rev. Neurosci.* **9**, 601-613. doi:10.1038/nrn2411
Erber, J., Kierzek, S., Sander, E. and Grandy, K. (1998). Tactile learning in the honeybee. *J. Comp. Physiol. A Sens. Neural Behav. Physiol.* **183**, 737-744. doi:10.1007/s003590050296
Erber, J., Pribbenow, B., Bauer, A. and Kloppenburg, P. (1993). Antennal reflexes in the honeybee: tools for studying the nervous system. *Apidologie* **24**, 283-296. doi:10.1051/apido:19930308
Fenster, C. B., Armbruster, W. S., Wilson, P., Dudash, M. R. and Thomson, J. D. (2004). Pollination syndromes and floral specialization. *Ann. Rev. Ecol. Evol. Syst.* **35**, 375-403. doi:10.1146/annurev.ecolsys.34.011802.132347
Fenske, M. P., Nguyen, L. A. P., Horn, E. K., Riffell, J. A. and Imaizumi, T. (2018). Circadian clocks of both plants and pollinators influence flower seeking behavior of the pollinator hawkmoth Manduca sexta. *Sci. Rep.* **8**, 1-13. doi:10.1038/s41598-018-21251-x
Goyret, J. (2010). Look and touch: multimodal sensory control of flower inspection movements in the nocturnal hawkmoth Manduca sexta. *J. Exp. Biol.* **213**, 3676-3682. doi:10.1242/jeb.045831
Goyret, J. and Kelber, A. (2011). How does a diurnal hawkmoth find nectar? Differences in sensory control with a nocturnal relative. *Behav. Ecol.* **22**, 976-984. doi:10.1093/beheco/arr078
Goyret, J. and Kelber, A. (2012). Chromatic signals control proboscis movements during hovering flight in the hummingbird hawkmoth Macroglossum stellatarum. *PLoS ONE* **7**, e34629. doi:10.1371/journal.pone.0034629
Goyret, J. and Raguso, R. A. (2006). The role of mechanosensory input in flower handling efficiency and learning by Manduca sexta. *J. Exp. Biol.* **209**, 1585-1593. doi:10.1242/jeb.02169
Goyret, J., Markwell, P. M. and Raguso, R. A. (2008a). Context- and scale-dependent effects of floral CO2 on nectar foraging by Manduca sexta. *Proc. Natl. Acad. Sci. USA* **105**, 4565-4570. doi:10.1073/pnas.0708629105
Goyret, J., Pfaff, M., Raguso, R. A. and Kelber, A. (2008b). Why do Manduca sexta feed from white flowers? Innate and learnt colour preferences in a hawkmoth. *Naturwissenschaften* **95**, 569-576. doi:10.1007/s00114-008-0350-7
Grimaldi, D. (1999). The co-radiations of pollinating insects and angiosperms in the cretaceous. *Ann. Mo. Bot. Gard.* **86**, 373-406. doi:10.2307/2666181
Haverkamp, A., Yon, F., Keesey, I. W., Mißbach, C., Koenig, C., Hansson, B. S., Baldwin, I. T., Knaden, M. and Kessler, D. (2016). Hawkmoths evaluate scenting flowers with the tip of their proboscis. *eLife* **5**, e15039. doi:10.7554/eLife.15039
Haverkamp, A., Li, X., Hansson, B. S., Baldwin, I. T., Knaden, M. and Yon, F. (2019). Flower movement balances pollinator needs and pollen protection. *Ecology* **100**, 1-11. doi:10.1002/ecy.2553
Huet, L. A., Schroeder, C. L. and Hartmann, M. J. Z. (2015). Tactile signals transmitted by the vibrissa during active whisking behavior. *J. Neurophysiol.* **113**, 3511-3518. doi:10.1152/jn.00011.2015
Johnson, S. D. (2012). Phylogenetic evidence for pollinator- driven diversification of angiosperms. *Trends Ecol. Evol.* **27**, 353-361. doi:10.1016/j.tree.2012.02.002
Kay, K. M. and Sargent, R. D. (2009). The role of animal pollination in plant speciation: integrating ecology, geography, and genetics. *Ann. Rev. Ecol. Evol. Syst.* **40**, 637-656. doi:10.1146/annurev.ecolsys.110308.120310
Kelber, A. (1997). Innate preferences for flower features in the hawkmoth Macroglossum stellatarum. *J. Exp. Biol.* **200**, 827-836.
Kelber, A. (2002). Pattern discrimination in a hawkmoth: innate preferences, learning performance and ecology. *Proc. R. Soc. B* **269**, 2573-2577. doi:10.1098/rspb.2002.2201
Kessler, D., Kallenbach, M., Diezel, C., Rothe, E., Murdock, M. and Baldwin, I. T. (2015). How scent and nectar influence floral antagonists and mutualists. *eLIFE* **4**, 1-16. doi:10.7554/eLife.07641
Kevan, P. G. and Lane, M. A. (1985). Flower petal microtexture is a tactile cue for bees. *Proc. Natl Acad. Sci. USA* **82**, 4750-4752. doi:10.1073/pnas.82.14.4750
Kier, W. M. and Smith, K. K. (1985). Tongues, tentacles and trunks: the biomechanics in muscular hydrostats. *Zool. J. Linn. Soc.* **83**, 307-324. doi:10.1111/j.1096-3642.1985.tb01178.x
Klein, A.-M., Vaissière, B. E., Cane, J. H., Steffan-Dewenter, I., Cunningham, S. A., Kremen, C. and Tscharntke, T. (2007). Importance of pollinators in changing landscapes for world crops. *Proc. R. Soc. B* **274**, 303-313. doi:10.1098/rspb.2006.3721
Kleinfeld, D., Ahissar, E. and Diamond, M. E. (2006). Active sensation : insights from the rodent vibrissa sensorimotor system. *Curr. Opin. Neurobiol.* **16**, 435-444. doi:10.1016/j.conb.2006.06.009
Kraaij, M. and Kooi, C. J. (2019). Surprising absence of association between flower surface microstructure and pollination system. *Plant Biol.* **22**, 177-183. doi:10.1111/plb.13071
Krenn, H. W. (1990). Functional morphology and movements of the proboscis of Lepidoptera (Insecta). *Zoomorphology* **110**, 105-114. doi:10.1007/BF01632816
Krenn, H. W. (2010). Feeding mechanisms of adult Lepidoptera: structure, function, and evolution of the mouthparts. *Annu. Rev. Entomol.* **55**, 307-327. doi:10.1146/annurev-ento-112408-085338
Mathis, A., Mamidanna, P., Cury, K. M., Abe, T., Murthy, V. N., Mathis, M. W. and Bethge, M. (2018). DeepLabCut: markerless pose estimation of user-defined body parts with deep learning. *Nat. Neurosci.* **21**, 1281-1289. doi:10.1038/s41593-018-0209-y
Mongeau, J.-M., Demir, A., Lee, J., Cowan, N. J. and Full, R. J. (2013). Locomotion-and mechanics-mediated tactile sensing: Antenna reconfiguration simplifies control during high-speed navigation in cockroaches. *J. Exp. Biol.* **216**, 4530-4541. doi:10.1242/jeb.083477
Ollerton, J., Winfree, R. and Tarrant, S. (2011). How many flowering plants are pollinated by animals? *Oikos* **120**, 321-326. doi:10.1111/j.1600-0706.2010.18644.x
Peng, F., Campos, E. O., Sullivan, J. G., Berry, N., Song, B. B., Daniel, T. L. and Bradshaw, H. D. (2019). Morphospace exploration reveals divergent fitness optima between plants and pollinators. *PLoS ONE* **14**, 1-12. doi:10.1371/journal.pone.0213029
Policha, T., Davis, A., Barnadas, M., Dentinger, B. T., Raguso, R. A. and Roy, B. A. (2016). Disentangling visual and olfactory signals in mushroom-mimicking Dracula orchids using realistic three-dimensional printed flowers. *New Phytol.* **210**, 1058-1071. doi:10.1111/nph.13855
Raguso, R. A. and Willis, M. A. (2005). Synergy between visual and olfactory cues in nectar feeding by wild hawkmoths, Manduca sexta. *Anim. Behav.* **69**, 407-418. doi:10.1016/j.anbehav.2004.04.015
Riffell, J. A., Lei, H., Christensen, T. A. and Hildebrand, J. G. (2009). Characterization and coding of behaviorally significant odor mixtures. *Curr. Biol.* **19**, 335-340. doi:10.1016/j.cub.2009.01.041
Riffell, J. A., Lei, H., Leif, A. and Hildebrand, J. G. (2013). Neural basis of a pollinator's buffet: olfactory specialization and learning in manduca sexta. *Science* **339**, 200-204. doi:10.1126/science.1225483
Roth, E., Hall, R. W., Daniel, T. L. and Sponberg, S. (2016). Integration of parallel mechanosensory and visual pathways resolved through sensory conflict. *Proc. Natl. Acad. Sci. USA* **113**, 12832-12837. doi:10.1073/pnas.1522419113
Saal, H. P. and Bensmaia, S. J. (2014). Touch is a team effort: Interplay of submodalities in cutaneous sensibility. *Trends Neurosci.* **37**, 689-697. doi:10.1016/j.tins.2014.08.012
Sane, S. P., Dieudonné, A., Willis, M. A. and Daniel, T. L. (2007). Flight Control in Moths. *Science* **315**, 863-866. doi:10.1126/science.1133598
Schütz, C. and Dürr, V. (2011). Active tactile exploration for adaptive locomotion in the stick insect. *Philos. Trans. R. Soc. B Biol. Sci.* **366**, 2996-3005. doi:10.1098/rstb.2011.0126
Skedung, L., Arvidsson, M., Chung, J. Y., Stafford, C. M., Berglund, B. and Rutland, M. W. (2013). Feeling small: exploring the tactile perception limits. *Sci. Rep.* **3**, 2617. doi:10.1038/srep02617
Solvi, C., Al-Khudhairy, S. G. and Chittka, L. (2020). Bumble bees display cross-modal object recognition between visual and tactile senses. *Science* **367**, 910-912. doi:10.1126/science.aay8064
Sponberg, S., Dyhr, J. P., Hall, R. W. and Daniel, T. L. (2015). Luminance-dependent visual processing enables moth flight in low light. *Science* **348**, 1245-1248. doi:10.1126/science.aaa3042
Stöckl, A. L., Ribi, W. A. and Warrant, E. J. (2016). Adaptations for nocturnal and diurnal vision in the hawkmoth lamina. *J. Comp. Neurol.* **524**, 160-175. doi:10.1002/cne.23832
Stöckl, A. L., Kihlström, K., Chandler, S. and Sponberg, S. (2017). Comparative system identification of flower tracking performance in three hawkmoth species

reveals adaptations for dim light vision. *Philos. Trans. R. Soc. B Biol. Sci.* **372**, 20160078. doi:10.1098/rstb.2016.0078

Stöckl, A. L., O'Carroll, D. C. and Warrant, E. J. (2020). Hawkmoth lamina monopolar cells act as dynamic spatial filters to optimize vision at different light levels. *Sci. Adv.* **6**, eaaz8645. doi:10.1126/sciadv.aaz8645

Theobald, J. C., Warrant, E. J. and O'Carroll, D. C. (2009). Wide-field motion tuning in nocturnal hawkmoths. *Proc. Biol. Sci. B* **277**, 853-860. doi:10.1098/rspb.2009.1677

Von Arx, M., Goyret, J., Davidowitz, G. and Raguso, R. A. (2012). Floral humidity as a reliable sensory cue for profitability assessment by nectar-foraging hawkmoths. *Proc. Natl. Acad. Sci. USA* **109**, 9471-9476. doi:10.1073/pnas.1121624109

Walton, R. E., Sayer, C. D., Bennion, H. and Axmacher, J. C. (2020). Nocturnal pollinators strongly contribute to pollen transport of wild flowers in an agricultural landscape. *Biol. Lett.* **16**, 20190877. doi:10.1098/rsbl.2019.0877

Wannenmacher, G. and Wasserthal, L. T. (2003). Contribution of the maxillary muscles to proboscis movement in hawkmoths (Lepidoptera: Sphingidae) - An electrophysiological study. *J. Insect Physiol.* **49**, 765-776. doi:10.1016/S0022-1910(03)00113-6

Whitney, H. M., Chittka, L., Bruce, T. J. and Glover, B. J. (2009). Conical epidermal cells allow bees to grip flowers and increase foraging efficiency. *Curr. Biol.* **19**, 948-953. doi:10.1016/j.cub.2009.04.051

Whitney, H. M., Bennett, K. M., Dorling, M., Sandbach, L., Prince, D., Chittka, L. and Glover, B. J. (2011). Why do so many petals have conical epidermal cells? *Ann. Bot.* **108**, 609-616. doi:10.1093/aob/mcr065

Zhang, C., Adler, P. H., Monaenkova, D., Andrukh, T., Pometto, S., Beard, C. E. and Kornev, K. G. (2018). Self-assembly of the butterfly proboscis: the role of capillary forces. *J. R. Soc. Interface* **15**, 20180229. doi:10.1098/rsif.2018.0229

Zhou, W., Kügler, A., McGale, E., Haverkamp, A., Knaden, M., Guo, H., Beran, F., Yon, F., Li, R., Lackus, N. et al. (2017). Tissue-specific emission of (E)-α-bergamotene helps resolve the dilemma when pollinators are also herbivores. *Curr. Biol.* **27**, 1336-1341. doi:10.1016/j.cub.2017.03.017

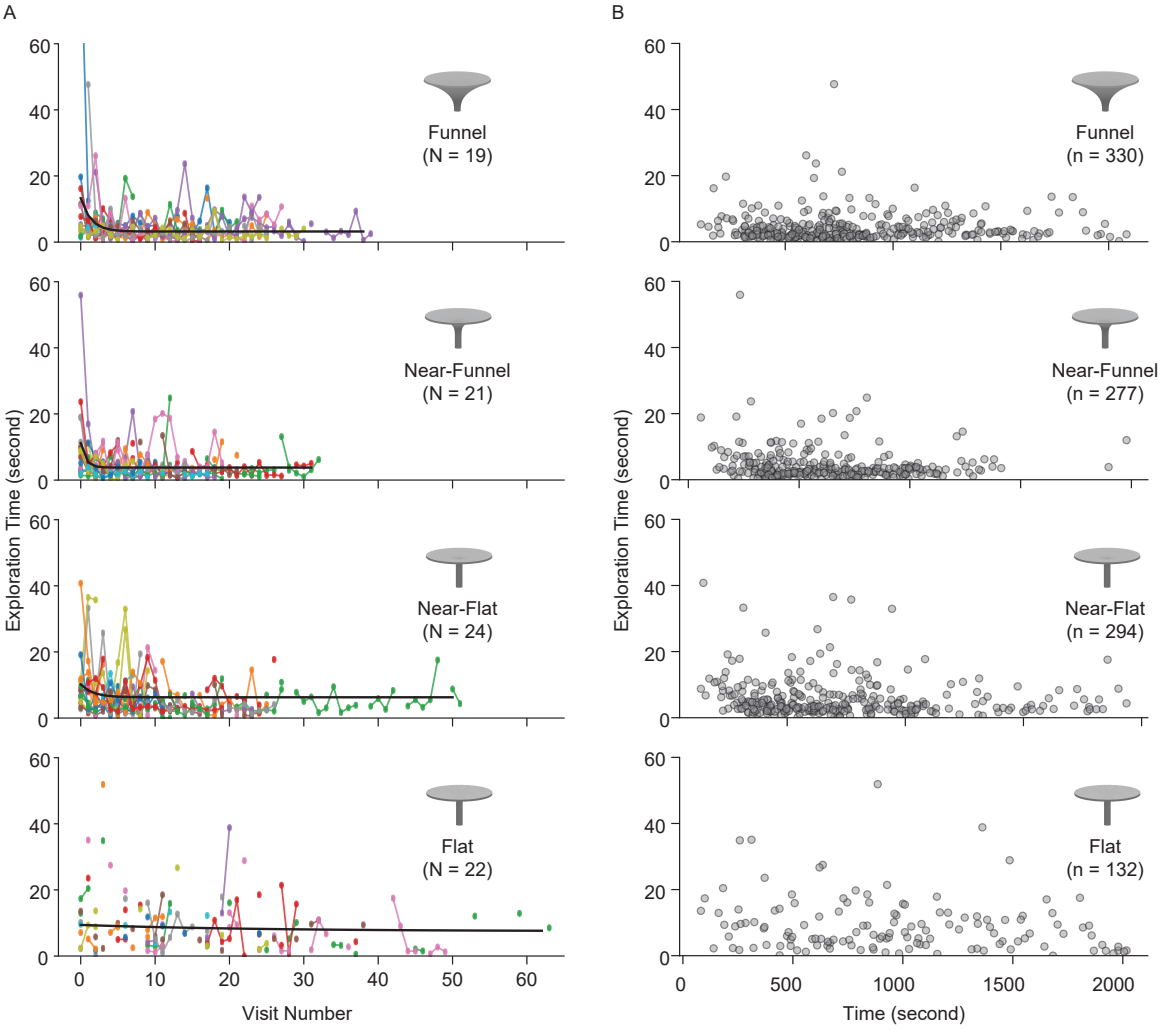

Figure S1: (A) Learning curves for individual moths across all floral shapes are plotted as versus visit number (panel A) and time (panel B). Each color in panel A is for a separate individual. The black solid line is the exponential fit to the data pooled across all moths as shown in Fig 2 in main MS. Each dot in panel B represents a single successful visit.

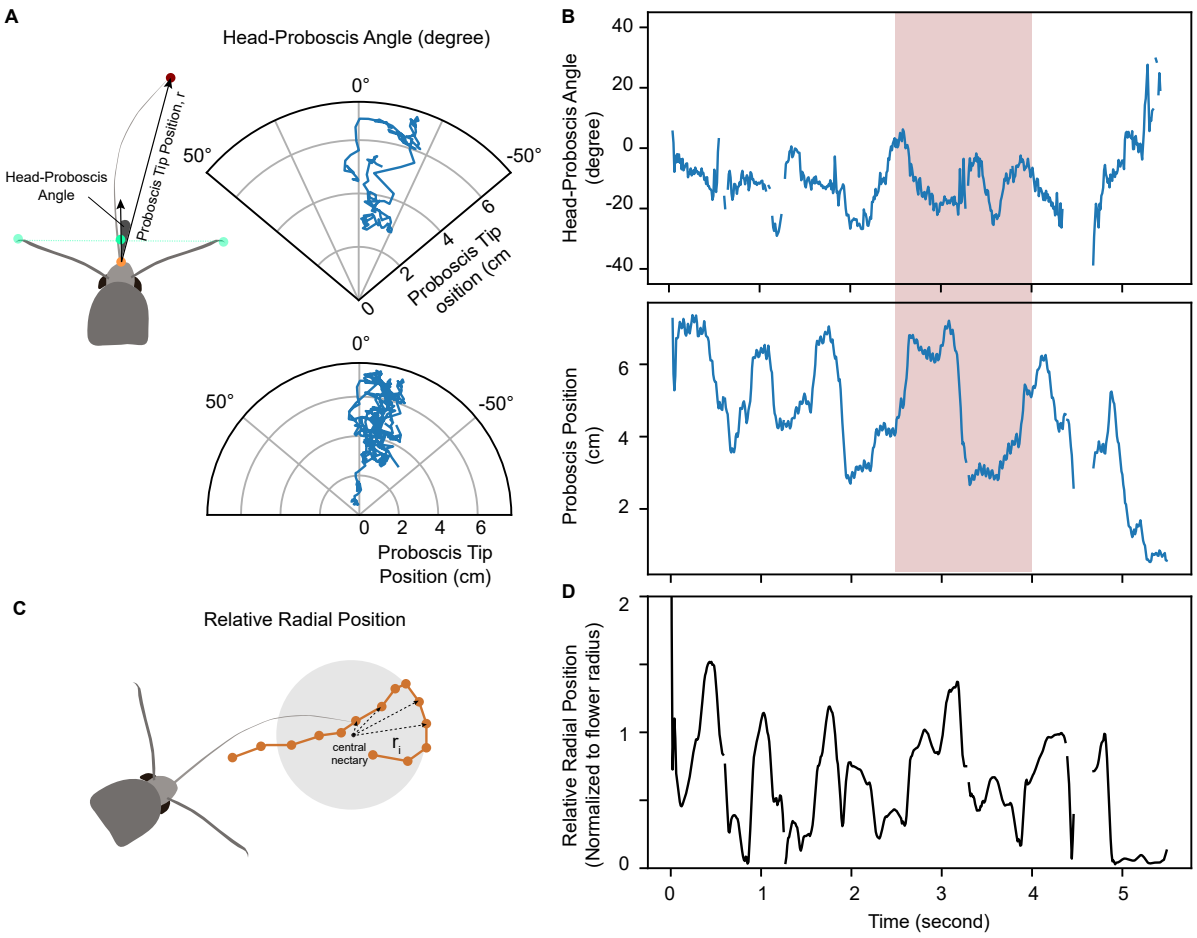

Figure S2: Proboscis mov ement relative to head. A) The cartoon on the left shows how we compute the angle and position of the proboscis tip relative to the head direction vector. The polar plots show the tracks of the proboscis tip relative to the head for a representative moth exploring the flat flower for the first visit. The track on top is a zoomed in view of the bottom track (in blue) B) Both the relative angle between the proboscis tip and head (top) and relative position of the tip from the head (bottom) varies as the moth (same visit as in A) explores the floral surface. The transparent red bar represents the track zoomed in A. C) The cartoon shows how we compute the relative radial position of the proboscis tip (relative to the flower radius) for a representative proboscis track (in orange). D) The proboscis tip position relative to the flower radius for the visit in A shows moths sweeping its proboscis from edge to center - center to edge repeatedly. Gaps in all tracks occur where the tracking error was large and hence not reliable.

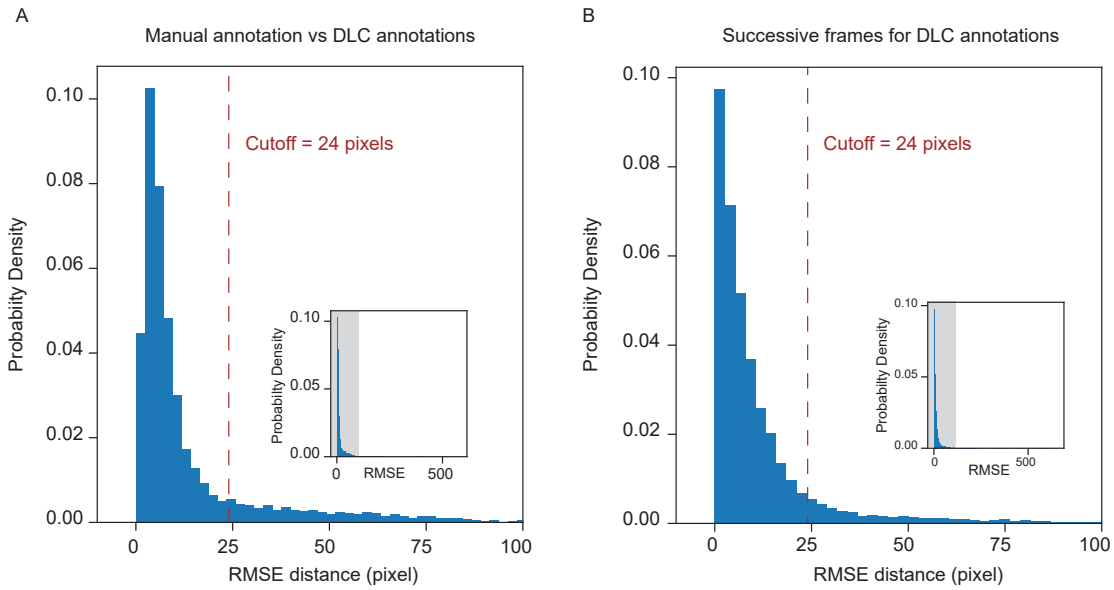

Figure S3: The probability density distribution for the root mean square error (RMSE) distance between the proboscis tip in A) manually annotated versus DeepLabCut (DLC) annotations and in B) successive frames for the DLC annotations are shown here. We manually annotated 6 videos comprising of 10308 frames. Based on the error comparing manual to DLC annotations (shown in A), we used a cut off of 24 pixels. If the distance between the proboscis tip on successive frames with DLC annotations (shown in B) was larger than this cutoff, the tracking data for that frame was dropped. With this cutoff, we could include 87.84% of our data. Inset shows the entire distribution with the grey bar highlighting the region that is zoomed in to visualize the cutoff pixel distance.

(a) Early - Later Visits Within Flowers

flower	**Kolmogorov-Smirnov test p value**
funnel	0.546
near-funnel	$1.05e^2$
near-flat	$2.41e^4$
flat	0.463

(b) Early Visits Across Flowers

flower pair	**Kolmogorov-Smirnov test p value**	**Kullback-Leibler Divergence**
funnel/near-funnel	0.992	0.001
funnel/near-flat	0.026	0.04
funnel/flat	0.003	0.17
near-funnel/near-flat	0.069	–
near-funnel/flat	0.010	–
near-flat/flat	0.128	–

(c) Later Visits Across Flowers

flower pair	**Kolmogorov-Smirnov test p value**	**Kullback-Leibler Divergence**
funnel/near-funnel	0.063	0.03
funnel/near-flat	0.393	0.005
funnel/flat	0.014	0.54
near-funnel/near-flat	0.342	–
near-funnel/flat	$2.26e^4$	–
near-flat/flat	$2.93e^3$	–

Table S1: Statistics for exploration times across flowers and visitsS

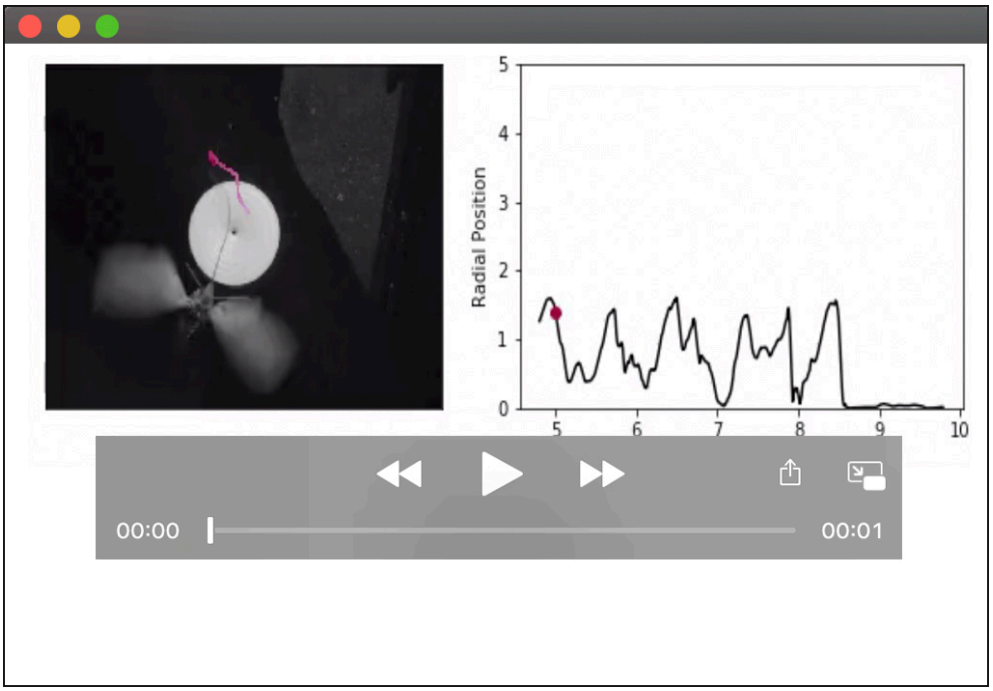

Movie 1: A moth exploring a slightly curved, near-flat flower with its pro-boscis during it's first visit.